Doi: 10.58414/SCIENTIFICTEMPER.2025.16.10.01

https://scientifictemper.com/

CASE STUDY

## AI Driven Approach in Smart Manufacturing in Bangladesh

Sirajum Munira Priety1\*, Farhan Bin Manjur2

#### **Abstract**

Predictive Maintenance (PdM) has become essential in smart manufacturing for reducing Downtime, improving efficiency, and cutting operational costs. The primary aim is to develop an Artificial Intelligence (AI) driven PdM framework for induction motors, leveraging IoT-based condition monitoring and time-series forecasting to estimate Remaining Useful Life (RUL) and enable intelligent maintenance scheduling. For this purpose, real-time Vibration and temperature data were collected from 2022 to 2024 using MPU-6050 sensors, followed by preprocessing, feature extraction, and fault trend analysis. The Prophet *algorithm*, known for handling seasonality and holiday effects, was employed for forecasting failure patterns and RUL estimation. Experimental analysis revealed distinct fault stages: unbalance, mechanical looseness, and bearing degradation; captured through Fast Fourier Transform (FFT) and time-domain features. Model validation across three axes showed strong performance with Coefficient of Determination (R²) up to 0.958, Root Mean Square Error (RMSE) as low as 0.110, and Mean Absolute Error (MAE) of 0.088, enabling accurate prediction of failure windows and proactive scheduling. However, limitations include a narrow dataset, reliance on two sensor modalities, and the exclusive use of Prophet, which struggles with highly non-linear dynamics. Future work would address these by incorporating hybrid AI models and multi-sensor fusion for improved prediction accuracy and scalability in large-scale deployments.

**Keywords:** Predictive maintenance, Artificial Intelligence (AI), Smart manufacturing, Cost reduction, Remaining Useful Life (RUL), Time-Series Forecasting.

#### Introduction

Predictive Maintenance (PdM) has emerged as leveraging loT-enabled condition monitoring to identify early indicators of spare degradation before failures occur (Soori *et al.*, 2023). Through conditional monitoring, loT sensors track parameters such as Vibration & temperature data in real time, producing large-scale data that reflects machine condition (Wen *et al.*, 2022). These data are essential for

<sup>1</sup>IWS Process Lead, Department of Secondary Manufacturing, Operations, British American Tobacco Bangladesh, Dhaka, Bangladesh.

<sup>2</sup>Coordinator & Analyst, Department of Primary Manufacturing, British American Tobacco Bangladesh, Dhaka, Bangladesh.

\*Corresponding Author: Sirajum Munira Priety, IWS Process Lead, Department of Secondary Manufacturing, Operations, British American Tobacco Bangladesh, Dhaka, Bangladesh, E-Mail: sirajum. priety@gmail.com

**How to cite this article:** Priety, S.M., Manjur, F.B. (2025). Al Driven Approach in Smart Manufacturing in Bangladesh. The Scientific Temper, **16**(10): 4834-4852.

Doi: 10.58414/SCIENTIFICTEMPER.2025.16.10.01

**Source of support:** Nil **Conflict of interest:** None.

shifting from reactive or preventive maintenance strategies to predictive approaches that minimize unplanned Downtime and enhance cost efficiency (Soori *et al.*, 2023). In smart factories, sensor-driven monitoring integrates seamlessly with Al forecasting frameworks to transform raw data into actionable insights (Wen *et al.*, 2022).

Among the forecasting techniques, the Prophet algorithm is becoming an increasingly prominent technique for remaining useful life (RUL) estimation by providing accurate and versatile RUL prediction from time-series sensor data (Ucar et al., 2024). It captures temporal patterns, seasonal trends, and can also handle missing values, a characteristic that makes Prophet a competent solution for industrial scenarios where data irregularities are the norm (Ucar et al., 2024). A manufacturer then uses this prediction to intervene only when degradation indications are detected, thus avoiding unnecessary preventive services that would otherwise reduce asset lifespan (Shamim & Ruddro, 2025). Hence, IoT-enabled monitoring coupled with Al-driven forecasting shortens maintenance and downtime schedules, fostering industrial operations that are safer, more dependable, and cheaper (Shamim & Ruddro, 2025). Here is Table 1 of industrial average savings achieved from Predictive Maintenance (PdM) across different sectors,

**Received:** 10/09/2025 **Accepted:** 02/10/2025 **Published:** 16/10/2025

Industry	Savings Area	Savings
Manufacturing sector in the US	Reduction of unplanned Downtime and maintenance costs	15-20%
Rail Sector in the UK	Elimination of Annual cost	£20 million equivalent
Automotive sector in Japan (Toyota)	Vehicle Uptime improvement and cost reduction	25-30%
Mining Operations in Brazil	Increase in equipment availability	15%
Energy sector in South Africa	Lowered equipment failure and maintenance costs	12% & 20%
The aerospace sector in the US	Increase in module availability	12%
The healthcare sector in the UK	Reduction in medical equipment downtime	22%
The semiconductor industry in Japan	Reduction in equipment failure and gain in efficiency	30% & 20%

Reduction of Downtime and proficiency in improvement

highlighting cost reductions, equipment availability improvements, and efficiency gains. These results demonstrate that PdM offers cross-sector operational gains in cost savings, spare availability, and reliability (Table 1).

#### **Predictive Maintenance Implementation**

The Agriculture industry in Brazil

Predictive maintenance (PdM) has emerged as a transformative strategy in modern industries, combining IoT-enabled monitoring, real-time data analytics, and Al-driven forecasting to anticipate equipment failures before they occur (Ayeni, 2025). Unlike traditional preventive methods, PdM enables targeted interventions based on actual asset conditions, thereby minimizing unplanned Downtime, reducing maintenance costs, and improving operational efficiency (Hossan *et al.*, 2025). By integrating continuous data acquisition with advanced decision-support systems (Wen *et al.*, 2022).

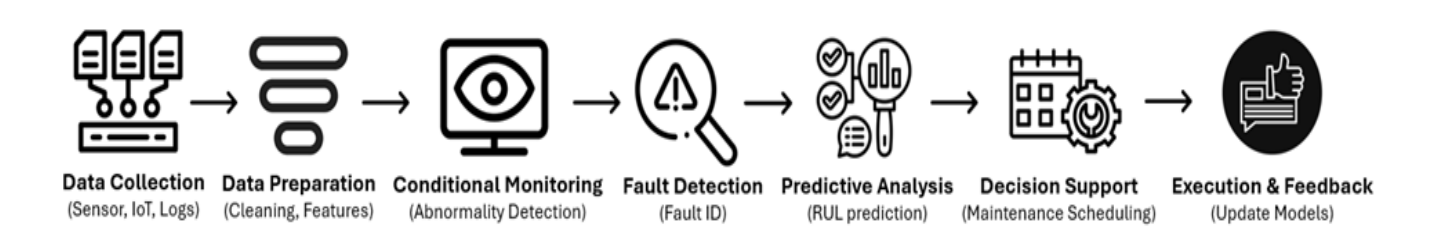
Figure 1 shows a comprehensive predictive maintenance (PdM) framework integrating IoT-enabled data acquisition, advanced analytics, and Al-driven decision-making. The fundamental process starts with data collection from sensors, IoT devices, and machine logs, ensuring continuous acquisition of various operational parameters like Vibration, Temperature, and pressure (Anny, 2023). Afterward, data preparation tools clean, preprocess, and extract the features from the data such that the criteria for quality are met and noise is removed (Subramanian, 2022). Now,

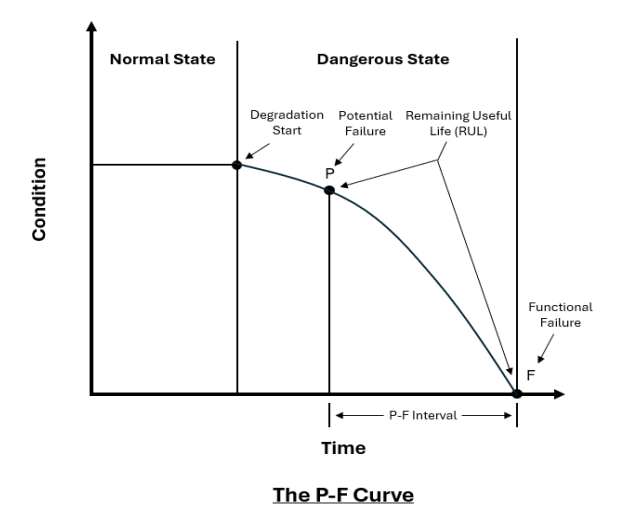
from the conditioning data to monitoring situations come various algorithms of design: from detecting early signs of abnormalities in machine behavior (Dhinakaran *et al.*, 2025).

17% & 12%

After this, the fault detection methods specify fault types, whereas predictive analysis applies algorithms to predict the Remaining Useful Life of the assets. The results are input into decision support systems, where maintenance schedules are optimized to reduce Downtime and costs. Execution and feedback complete the loop by updating the model with real-world outcomes, which enhances its accuracy with time. The sequence is closely aligned to the PdM architectures conceptualized very recently in the literature, where IoT, AI, and feedback loops are integrated for continuous evolution (Wen et al., 2022) (Figure 1).

Here in Figure 2, the P–F curve illustrates how spares' condition declines over time, moving from a normal state to a dangerous state before reaching functional failure (Bousdekis *et al.*, 2019). The interval between potential failure (P) and functional failure (F) is critical for estimating the Remaining Useful Life (RUL), which indicates how long the spare can operate before failure occurs (Bousdekis *et al.*, 2019). Predictive maintenance focuses on identifying the onset of degradation to accurately predict RUL and schedule maintenance within the P–F interval (Bousdekis *et al.*, 2019). This approach reduces Downtime, avoids costly stoppages, and optimizes maintenance planning (Bousdekis *et al.*, 2019) (Figure 2).





. . . . . . .

Figure 2: P-F Curve

## Role of AI in PdM

Artificial Intelligence (AI) strengthens predictive maintenance (PdM) by merging IoT sensor data, historical failure records, and real-time condition monitoring to enable precise fault detection and timely interventions (Emma, 2025, and Baroud *et al.*, 2025). In manufacturing, PdM frameworks integrate three core elements: condition monitoring sensors, IoT data acquisition, and predictive algorithms (Pejić Bach *et al.*, 2023). Condition monitoring captures real-time parameters such as Vibration and Temperature, which are processed to detect irregularities and predict Remaining Useful Life (RUL) (Sekar *et al.*, 2025). IoT systems connect these assets to centralized platforms for data storage, preprocessing, and analytics, ensuring continuous visibility of equipment condition (Sivakumar *et al.*, 2023).

Figure 3 depicts an Al-driven heuristic approach for PdM, wherein IoT-enabled data acquisition prepares sensor measurements of Vibration and Temperature (Emma, 2025). The captured readings form a training dataset for supervised or unsupervised modeling (Baloch et al., 2025). In data processing, cleaning, normalization, and feature extraction improve the signal quality (Ahadov et al., 2024). Early fault detection is implemented to detect early degradation before failure (Hosseinzadeh et al., 2023). The alarm logic and thresholds set the setpoints, triggering an alert whenever limits are breached (Pejić Bach et al., 2023). Realtime condition monitoring would continue to examine the health of spares in view of these thresholds (Subramanian, 2022). Equipment forecasting is carried out by applying the Prophet time-series model on historical trends (Syed et al., 2025). The forecast then assists in Remaining Useful Life (RUL) estimation, through which preemptive interventions could be carried out (Emma, 2025). Lastly, maintenance scheduling is implemented to align PdM actions with the production plan so as to minimize Downtime and initiate resource optimization (Pejić Bach et al., 2023) (Figure 3).

## **Enhancing Predictive Maintenance with the Proph**et algorithm

The Prophet algorithm provides distinct advantages for time-series datasets that exhibit seasonal patterns, holidays, and other recurring effects (Anand et al., 2024, and Chitwadgi, 2024). Unlike traditional models, Prophet is designed with flexible components that can adapt to the inherent complexities of real-world data, thereby improving both interpretability and forecasting accuracy (KC & Rone, 2024). The mathematical formulation of Prophet can be expressed as:

#### Adaptive seasonality

Models complex seasonal patterns using Fourier series, capable of capturing variations across different frequencies and magnitudes.

## Holiday effects

Prophet effectively incorporates holidays and dedicated events, which are often overlooked in conventional forecasting methods (Manandhar *et al.*, 2024).

#### Robust anomaly detection

Prophet robustly manages outliers and missing values with resilience, minimizing their negative impact on predictions.

## Ease of implementation and adjustability

Provides user-friendly hyperparameter tuning, making the model highly adaptable across diverse datasets (Belim *et al.*, 2024).

This research aims to develop an Al-driven predictive maintenance (PdM) framework for induction motors in smart manufacturing by integrating loT-based condition monitoring with the Prophet time-series forecasting algorithm to predict failures and estimate Remaining Useful Life (RUL). The scope includes analyzing vibration and temperature data to capture degradation patterns, seasonal variations, and early fault indicators, as well as implementing forecasting-based maintenance scheduling. It also covers sensor-based data acquisition, feature extraction, Prophet model training, and the development of a hybrid dashboard for real-time decision-making.

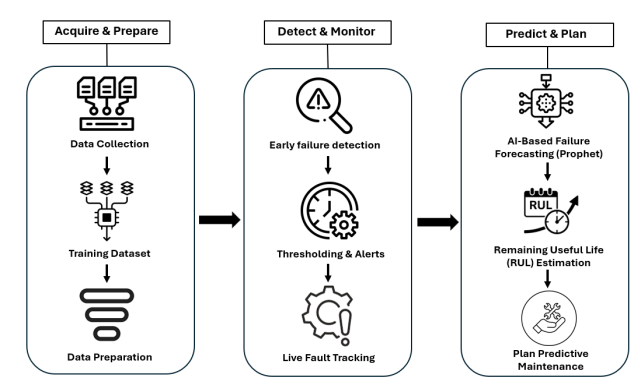


Figure 3: Framework of Al-driven PdM

The novelty of this work lies in modeling both seasonal and event-based operational patterns, such as holiday shutdowns and post-holiday ramp-up effects, within the PdM framework using the Prophet algorithm, an aspect often overlooked in existing studies. Additionally, the study introduces a hybrid dashboard that integrates real-time sensor monitoring with predictive insights for RUL-based scheduling, while incorporating lead-time-aware maintenance planning for practical industrial deployment.

This research contributes by proposing a structured Al-based PdM framework that combines IoT-driven condition monitoring with advanced time-series forecasting for accurate RUL prediction. It enhances predictive maintenance by incorporating seasonal and operational trends into forecasting, introduces a hybrid dashboard for visualization and decision support, and establishes a scheduling approach that accounts for lead time and buffer requirements. These contributions collectively offer a practical and scalable solution for improving reliability, reducing Downtime, and optimizing cost in smart manufacturing environments.

The latest research in predictive maintenance (PdM) emphasizes advanced AI frameworks that integrate domain knowledge, data, and models to enhance decision-making in manufacturing (Lee & Su, 2025). These frameworks leverage benchmark datasets from PHM competitions to validate PdM techniques, thereby promoting standardized performance evaluations (Lee & Su, 2025). However, recent studies reveal gaps, including inadequate classification of supervised machine learning methods and limited comparative analysis between synthetic and real-world datasets (Guidotti et al., 2025). Further improvements have been achieved through Al-integrated PdM frameworks combining IoT and machine learning models. These systems demonstrated up to 92% accuracy in failure prediction and reduced Downtime by 35%, though limitations persist in terms of hybrid AI architectures and broader IoT coverage (Abdulrazzq et al., 2024). While integration with ERP systems has enhanced equipment effectiveness, scalability, interpretability, and computational complexity remain key challenges (Abdulrazzq et al., 2024).

Practical implementations underscore the tangible benefits of PdM across global industries. For instance, the UK rail industry realized £20 million annual savings and a 10% improvement in train reliability, while Toyota in Japan reduced maintenance costs by 25% and increased vehicle uptime by 30% (Kairo, 2024). Similarly, Brazil's mining sector improved equipment availability by 15% and lowered maintenance expenditure by 10%, and South Africa's energy sector experienced a 12% reduction in equipment failures alongside 20% lower maintenance costs (Kairo, 2024). The rise of Industry 4.0 has been a major driver of this transformation, shifting maintenance strategies toward data-driven, intelligent PdM solutions (Soori et al., 2023). IoT technologies play a central role by continuously

monitoring parameters such as pressure, Sound, Vibration, and Temperature in industrial systems (Soori *et al.*, 2023).

Nevertheless, full integration remains hampered by challenges like device interoperability, high energy consumption, and data security risks (Soori et al., 2023). Many PdM systems function primarily as alert mechanisms rather than enabling comprehensive predictive scheduling, leaving a gap between real-time monitoring and actionable maintenance strategies (Zonta et al., 2020). Earlier research laid the foundation for these advancements. Zonta et al. (2020) highlighted the capability of PdM to reduce unplanned Downtime and optimize manufacturing schedules through Al-based forecasting models and realtime sensor data. Despite these strengths, they observed that most PdM applications failed to bridge the gap between condition monitoring and strategic maintenance planning (Zonta et al., 2020). At the same time, foundational studies stressed unresolved issues in PdM implementation.

## Research Gap

This section shows the research gaps based on the previous studies.

- between condition monitoring and ongoing maintenance scheduling, limiting their capacity for optimizing operational Downtime and allocation of resources. Even though these solutions are very good at identifying anomalies within real-time situations, they do not convert these observations into viable longer-term maintenance strategies capable of averting future failure. This lags considerably behind the industry's capacity for minimizing unexpected shutdown and general operational efficiency (Zonta et al., 2020).
- In addition, the Prophet algorithm, which has been promising for time-series forecasting applications within a variety of fields, remains underdeveloped for cost-oriented PdM applications within smart manufacturing facilities. Even though Prophet proved capable of dealing with seasonal trends within irregular data, there has been insufficient development of integrating it into cost-saving strategies for the purpose of maximizing uptime and system reliability (Lee & Su, 2025).
- In addition, the field lacks adequate comparative studies
  of PdM performance within synthetic and real-world
  databases. This imbalance is a significant difficulty since
  synthetic databases, although controlled, do not reflect
  the complexity and noise within real-world applications.
  This hinders the possibility of extrapolating the results
  of such databases to the real situation within industries,
  where unpredictability and irregularities within the
  data are the order of the day. As such, the scalability
  and robustness of many PdM models suffer in such
  applications within the industries whenever they

consider the large scale on which the industries operate.

In addition, these PdM solutions incorporating the use of Al suffer from computational bottlenecks whenever they deal with the issue of high volumes of data and the reality of required real-time computations within enormous distributed applications. These limitations make it difficult for such solutions to be practically implemented within industries whose applications are heavy and call for fast decision-making (Guidotti et al., 2025).

#### Research Questions based on this research:

- How does the sampling rate of real-time condition-monitoring data (e.g., Vibration + Temperature) influence the predictive accuracy of PdM forecasting models?
- How accurately can a Prophet-based forecasting model predict critical condition-monitoring parameters (e.g., vibration, temperature) in real time compared with traditional PdM models such as ARIMA and LSTM?
- What percentage reduction in unplanned Downtime and total maintenance cost can be achieved when real-time condition monitoring is combined with Prophet-driven forecasts versus a reactive or calendar-based maintenance strategy?
- Can a hybrid framework (dashboard), combining Prophet forecasts with anomaly-detection score, improve interpretability and decision confidence for maintenance schedulers?

## **Materials and Methods**

The research is based on the implementation of predictive maintenance using sensor-based condition monitoring for early failure detection of motor vibration and Temperature. As part of this review, raw data collected from sensor hardware were analyzed, the datasets were evaluated, and

the primary data were trained using an Al model to predict future failures.

## **Experiment Description**

The motor's real-time Vibration and temperature failure simulation experiment was conducted using an Enerzyz Vibro-Temperature wired sensor (Model: MPU-6050), which was deployed for continuous condition monitoring of a 0.75 KW, 50 Hz, 1440 RPM induction motor throughout the 2024 operational period. The sensor, comprising a 3-axis accelerometer, gyroscope, and internal temperature sensor, was rigidly mounted to the motor housing using vibration-damping adhesive to ensure stable signal acquisition and minimize noise from extraneous sources. The wired configuration ensured stable signal transmission and reduced wireless interference during prolonged data acquisition. Figure 4 below explains the process of securely mounting the MPU-6050 sensor to the motor housing using vibration-damping adhesives to maintain contact stability and minimize extraneous noise (Figure 4).

Table 2 shows the concise summary that connects the Enerzyz Vibro-temperature wired sensor data acquisition process with its technical features, as per the provided details (Table 2):

A digital low-pass filter with a 94 Hz cutoff was applied to the vibration channels to suppress high-frequency noise and electrical interference. From the filtered signals, time-domain features including RMS acceleration, peak amplitude, kurtosis, and crest factor were computed over fixed 1-second analysis windows. Frequency-domain analysis using FFT was performed periodically to detect dominant fault frequencies.

Data collection spanned multiple seasonal and operational variations, enabling the capture of long-term degradation trends as well as short-term transient anomalies. This temporal resolution made it possible to observe both

Table 2: Enerzyz Vibro-temperature wired sensor data acquisition process parameters

	, , , , , , , , , , , , , , , , , , , ,	
Category	Specification/Process	
Product (Model)	MPU-6050 (3-axis accelerometer + gyroscope + internal temperature sensor)	
Mounting Method	Fixed to the motor housing with vibration-damping adhesive for stable measurement	
Power Supply	3.3 V regulated	
Communication	I <sup>2</sup> C interface at 400 kHz for reliable, low-latency data transfer	
Accelerometer Range	±8 g for capturing a wide range of vibration amplitudes	
Gyroscope Range	±1000 °/s rotational speed and movement tracking	
Sampling Frequency	200 Hz for vibration data; 1 Hz for temperature monitoring	
Signal Filtering	Digital low-pass filter, 94 Hz cutoff to remove high-frequency	
Time-Domain Features	Extraction of RMS, peak amplitude, kurtosis, crest factor for condition monitoring	
Frequency-Domain Analysis	Fast Fourier Transform (FFT) to specify fault-specific frequency components	
Baseline Reference	Healthy (Normal Phase) operational data used for threshold calibration and fault comparison	

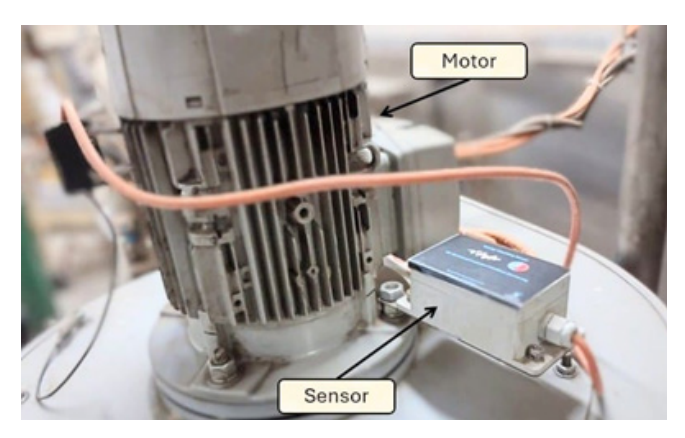


Figure 4: Motor simulation

cyclical patterns (e.g., seasonal load changes) and secondlevel variations in machine behavior. The acquired datasets were logged in the acquisition unit's internal memory and periodically exported in CSV format for offline processing. Each CSV file contained timestamped records of:

- Axial, radial, and tangential acceleration values (m/s²),
- Gyroscope angular velocity readings (°/s)
- Corresponding temperature measurements (°C).

This standardized CSV structure facilitated seamless integration with statistical analysis tools (MATLAB, Python) for both real-time monitoring and historical trend analysis, ensuring reproducibility and scalability of the predictive maintenance framework.

## Methodology

The study focuses on implementing a Smart Predictive maintenance framework for an Induction motor in a Manufacturing unit. This combines three stages as shared below in Figure 5: initially, real-time condition monitoring of the test motor via a 6-axis motion tracking wired sensor network, identifying RUL (Remaining Useful Life) and determining threshold crossing point using the Prophet algorithm model developed by Facebook (meta), and finally scheduling PdM based on forecasting results (Figure 5).

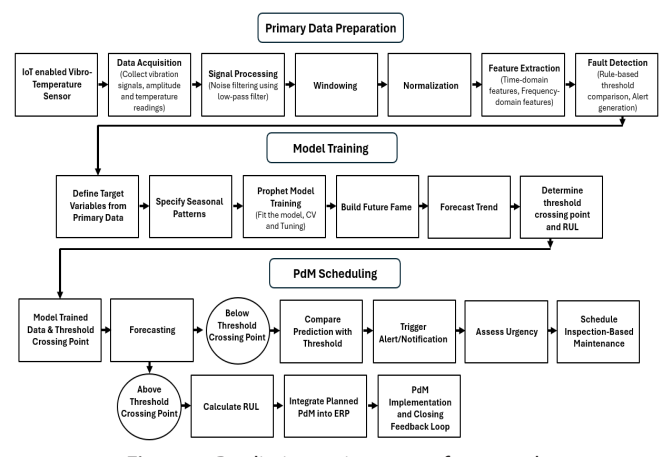


Figure 5: Predictive maintenance framework

## **Experimental Analysis (Primary Data)**

This research experiment explains two phases of motor's condition: normal and failure stage from sensor-based condition monitoring results.

 Induction Motor operated under normal conditions (real-time monitored data without fault indication):
 Table 3 includes temperature signals from condition monitoring of the year 2022.

Table 3 shows the real-time monitored parameters of the induction motor, which include Temperature, Vibration, Speed, and Sound of the motor. Table 3 depicts the realtime monitored data when a motor is operating under normal conditions, without any fault, and typically includes a range of parameters and metrics that indicate the health and performance of the motor. For example, in Table 3, the average Temperature is noted as 30.22558°C, Sound is noted as 71.523 dB, Vibration (acceleration) is observed between +-2 m/s2 and Speed is indicated as 1470 RPM, all these data were below the test set conditions (Temperature <35°C, Sound <75dB, Vibration with +-2 m/s2 and Speed <1500 RPM). From these values, it is validated that the motor is operating without any fault. These data are crucial for ensuring smooth operation and early detection of any potential issues. From the analyzed data, motor failure can be predicted based on the trained dataset. If any of the four parameters fail to achieve the normal value, the motor is considered to be in a fault stage; otherwise, it operates under normal conditions (Table 3).

Induction Motor under faulty condition (real-time monitored data with failure indication): Table 4 includes only temperature signals above threshold (> 35 °C) from condition monitoring of August 2022.

Table 4 depicts the real-time monitored data of the fault motor. Real-time monitored data of a faulted motor provides crucial insights into the abnormal conditions (mechanical looseness, bearing fault, misbalancing) and issues affecting its operation. From the above data, the motor failure can be predicted according to the trained dataset. For example, in Table 4, Temperature is noted as average 39.3889°C, Sound is noted as 76.6982 dB, Vibration is observed above  $\pm$  2.164 m/s2, and Speed is indicated as 1456 RPM, all of which exceeded the test set conditions (Temperature >35°C, Sound >75dB, Vibration >+-2 m/s2, and RPM<1500). From these values, it is observed that the motor is operating without any abnormalities such as mechanical looseness or bearing fault. These data are crucial for identifying early detection of any potential failure. From the analyzed data, motor failure can be predicted according to the trained dataset, and faults can be rectified based on inspection. Since most of the four parameters fail to achieve the normal threshold, the motor is considered to be in a fault stage; otherwise, it operates under normal conditions (Table 4).

Table 3: Real-time monitoring Parameters

- Table 51 flear time morntoring ratameters					
Temperature ©	Vibration (m/s2)	Sound (dB)	Motor RPM	Motor's Condition	
28.241	0.139	71.320	1471.350	Normal	
27.421	-0.106	71.240	1471.520	Normal	
33.297	0.048	71.830	1470.340	Normal	
28.246	-0.086	71.320	1471.350	Normal	
30.078	-0.086	71.510	1470.980	Normal	
27.865	0.042	71.290	1471.430	Normal	
29.877	-0.194	71.490	1471.020	Normal	
31.708	0.166	71.670	1470.660	Normal	
32.564	-0.182	71.760	1470.490	Normal	
34.344	0.061	71.930	1470.130	Normal	
29.796	-0.177	71.480	1471.040	Normal	
30.078	0.152	71.510	1470.980	Normal	
30.276	-0.165	71.530	1470.940	Normal	
30.304	0.072	71.530	1470.940	Normal	
29.959	-0.130	71.500	1471.010	Normal	
29.102	0.090	71.410	1471.180	Normal	
27.999	-0.120	71.300	1471.400	Normal	
31.697	0.049	71.670	1470.660	Normal	
29.981	-0.077	71.500	1471.000	Normal	
31.662	-0.077	71.670	1470.670	Normal	

## **Vibration Data Analysis**

The vibration data of the test motor was collected in real time during 2022-2024 condition monitoring experiments. Accelerometers were mounted on the motor to capture vibration signals under different operating conditions. This data was analyzed to investigate the signal characteristics of motor failure in 4 stages. To evaluate the fault signatures from acceleration (m/s2), vibration signals from each axis were compared to a  $\pm 2.0$  m/s² threshold derived from both normal and abnormal stages graphs (Figures 6 and 7).

#### Normal stage

The Y-axis signal remains compact and sub-threshold: most samples lie within  $\pm 1.0$  m/s<sup>2</sup>; only rare, short spikes

approach the  $\pm 2.0$  m/s<sup>2</sup> lines (Figure 6). According to the planned-based inspection, the acceleration signal between the threshold band means the motor is actuating at its regular condition without any mechanical abnormality such as looseness, misalignment, or bearing distress (Figure 6).

#### Abnormal Stage

To better compare acceleration values across different time spans, an abnormal moment throughout the total duration was uniformly selected (shown in Figure 7). An alarm band of ±2.0 m/s<sup>2</sup> was applied to the time-domain vibration signal. In the failure window (~0.1–1.9 sec), the tangential (Y) acceleration repeatedly crosses this band and remains outside it for extended periods. Here, the spikes reached roughly +4.0 m/s<sup>2</sup> and -4.5 m/s<sup>2</sup>, giving a much larger peak-to-peak (~4–4.5 m/s<sup>2</sup>) and visibly higher overall energy (RMS). This pattern is impulsive (many sharp bursts), which is typical of developing mechanical problems such as looseness, misalignment, or bearing distress. The increase in spikes is due to the gradual loss of lubrication, leading to a reduction of oil film thickness and increased wear between the rolling elements of the motor. Therefore, the acceleration band above threshold means the motor is no longer vibrating within acceptable limits and is at high risk of unplanned stoppage unless inspected and repaired (e.g., alignment check, relubrication, or bearing replacement) (Figure 7).

Similarly, the acquired time-domain signals were then converted into the frequency domain using the Fast Fourier Transform (FFT), enabling a detailed evaluation of vibration characteristics across four distinct fault stages: Normal, Unbalancing, Mechanical Looseness, and Bearing Fault as shown in Figure: 8. The FFT plots provide insights into both the amplitude (Y-axis) and the frequency (X-axis) of vibration peaks, which are critical indicators for diagnosing fault type and severity. The severity and type of each fault can be evaluated by analyzing both the amplitude of vibration peaks and their position on the frequency spectrum. According to the Normal Stage of Figure 8, the vibration spectrum shows evenly distributed low-amplitude peaks, all remaining below the 0.1 threshold line. The absence of dominant peaks indicates stable operation without any

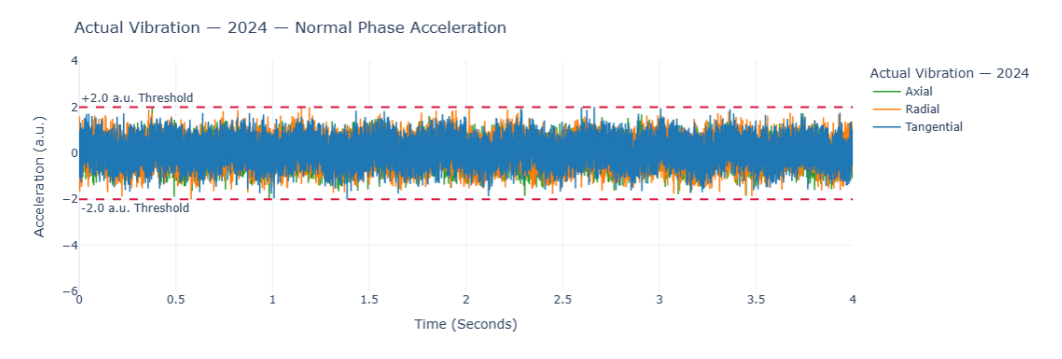


Figure 6: Normal Phase Acceleration

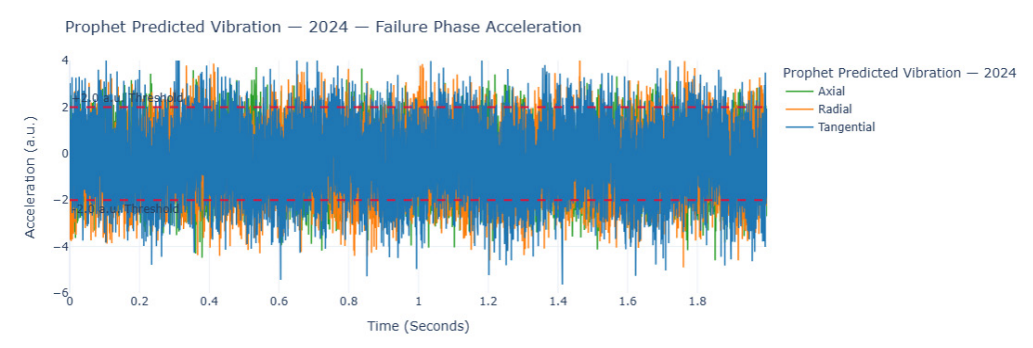


Figure 7: Failure Phase Acceleration

mechanical abnormalities. By monitoring the condition of an ideal motor, comparisons can be made between motors under fault conditions and that of a perfect motor (Figure 8).

#### Unbalancing

Based on the data presented in Figure 8, several peaks appear to be present at the Unbalancing (b) stage. The most notable peak is at 90 Hz, and other dominant peaks at ~70 Hz and ~90 Hz, with the amplitude up to 0.17. Compared to the 20-30 Hz peak seen in Normal Stage (a), which displays the motor operating under normal conditions, the 60-70 Hz peak of Unbalancing stage (b) shows a substantial increase in

Table 4: Monitoring parameters of Fault Motor

Temperature ©	Vibration (m/s2)	Sound (dB)	Motor RPM	Motor's condition	
39.090	0.351	75.270	1453.640	Abnormal	
35.414	-0.321	72.330	1468.350	Abnormal	
35.718	0.272	72.570	1467.130	Abnormal	
37.160	-0.292	73.730	1461.360	Abnormal	
39.146	0.317	75.320	1453.420	Abnormal	
38.568	-0.306	74.850	1455.730	Abnormal	
38.993	0.322	75.190	1454.030	Abnormal	
37.123	-0.263	73.700	1461.510	Abnormal	
37.550	0.286	74.040	1459.800	Abnormal	
38.545	-0.369	74.840	1455.820	Abnormal	
38.404	0.234	74.720	1456.380	Abnormal	
39.240	0.378	75.390	1453.040	Abnormal	
39.546	-0.281	75.640	1451.820	Abnormal	
38.720	0.292	74.980	1455.120	Abnormal	
39.599	-0.253	75.680	1451.610	Abnormal	
38.810	-0.236	75.050	1454.760	Abnormal	
39.080	0.235	75.260	1453.680	Abnormal	
38.758	-0.384	75.010	1454.970	Abnormal	
39.105	-0.236	75.280	1453.580	Abnormal	
38.885	0.249	75.110	1454.460	Abnormal	

amplitude. Additionally, the overall noise in the Unbalancing (b) phase appears to have changed. The conditions are characterized by sharp, distinct peaks at the fundamental running frequency (1× RPM) and sometimes its harmonics (2). To summarize, in the FFT spectrum, two strong peaks exceed the 0.1 threshold, confirming the presence of rotor unbalance.

#### Mechanical looseness

The FFT spectrum at the Mechanical Looseness stage (c) shows (as per Figure 8) multiple dominant peaks across the frequency range of 110–140 Hz. Several peaks rise above the 0.1 amplitude threshold, with the most notable ones reaching values between ~0.15 and 0.18. Compared to the Normal Stage (a), where vibration peaks remain below 0.07 and evenly distributed within the 20-30 Hz region, the Mechanical Looseness stage clearly demonstrates a broader and more irregular frequency response between 90 and 150 Hz. The presence of harmonics and sidebands at multiples of the fundamental frequency further supports the looseness condition. These peaks are not isolated but spread across higher frequencies, which reflects unstable contact points or loosened components in the motor structure. To summarize, the FFT spectrum for Mechanical Looseness is characterized by multiple harmonics, broad frequency energy distribution, and amplitudes exceeding the 0.1 threshold, confirming the presence of looseness-related vibration behavior.

## Bearing fault

As shown in Figure 8, the Bearing Fault stage (d) demonstrates a distinct vibration pattern compared to the Normal Stage (a). The FFT spectrum shows several irregular peaks concentrated in the higher frequency range of 180–200 Hz, with amplitudes rising to ~0.20, well above the 0.1 threshold. Unlike the Normal Stage, where peaks remain below 0.07 and evenly distributed, the Bearing Fault stage displays a raised noise floor and multiple high-frequency peaks that do not align with simple harmonics of the running Speed or with typical unbalance/mechanical looseness signatures. This irregular spectral behavior is a strong indicator of bearing degradation, likely due to lubrication failure or physical damage of rolling elements. When compared to the

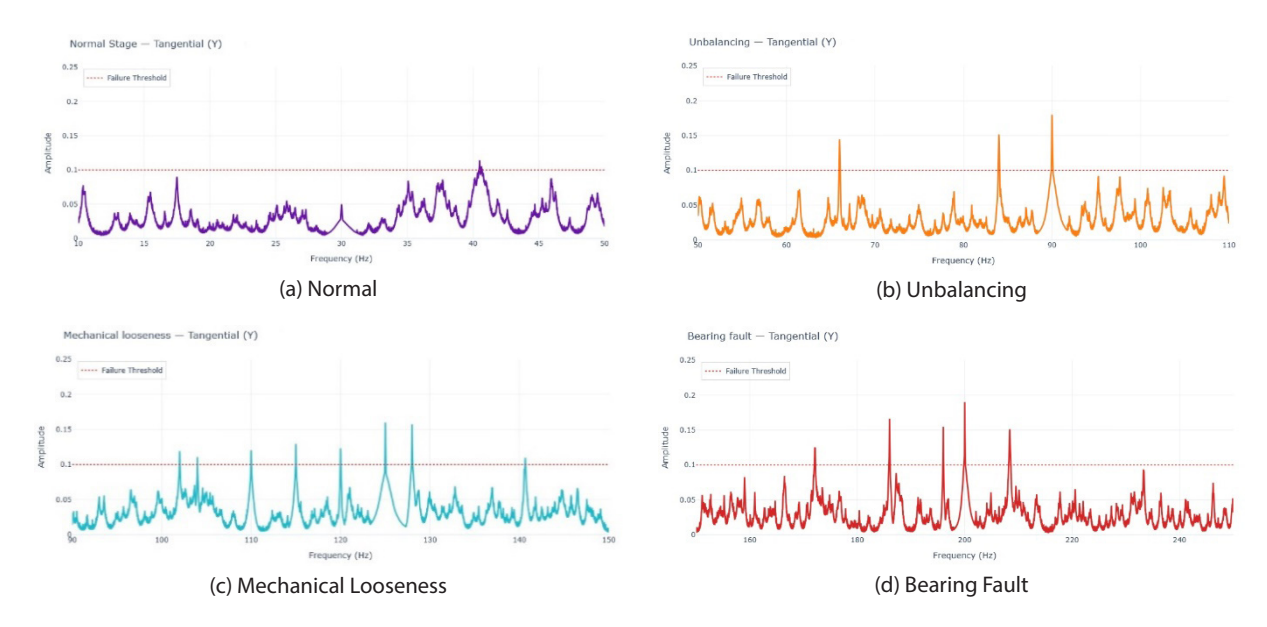


Figure 8: Distinct Fault Stages

spectrum recorded under healthy conditions (Normal Stage), it becomes evident that the motor's vibration response has undergone substantial change and is no longer stable. Such results suggest two possibilities: either there are inaccuracies in the recorded data, or the bearing has already advanced to a severe fault stage (stage four of failure). In summary, the Bearing Fault stage is characterized by high-frequency resonance, irregular peak distribution, elevated amplitude, and a raised noise floor, all of which confirm significant bearing deterioration.

#### Real-time Temperature Analysis

Insufficient lubrication induces additional friction and wear within motor bearings. Since frictional heating is a primary contributor to surface temperature rise, temperature monitoring becomes a critical diagnostic tool for identifying incipient bearing faults. Figure 9 illustrates the half-yearly thermal profile of the test motor, where surface temperature was continuously tracked against a control limit of 35 °C, established from prior failure events exceeding this threshold.

Between June and July, the motor operated within a relatively stable thermal band of 28-38 °C, with a low drift rate ( $\approx 0-0.1$  °C/day). A pronounced thermal excursion occurred in mid-August, when the Temperature escalated sharply to  $\sim 44$  °C, classified as a failure event before returning to baseline following corrective intervention. This sharp rise highlights the cumulative effect of progressive lubrication loss: as oil film integrity deteriorates, tribological interactions and bearing surface degradation intensify, resulting in a sudden surge in heat generation. The system then stabilized back to 27-30 °C for the remainder of the monitoring period (Figure 9).

To better resolve the pre-failure dynamics, a two-week window preceding the August excursion was analyzed (Figure 10). During this interval, motor surface temperature increased monotonically from ~28 °C to ~36–37 °C, crossing the 35 °C threshold around August 12–13. This gradual escalation reflects the early phase of lubrication degradation, where partial oil loss is insufficient to cause catastrophic friction but induces measurable incremental heating (Figure 10).

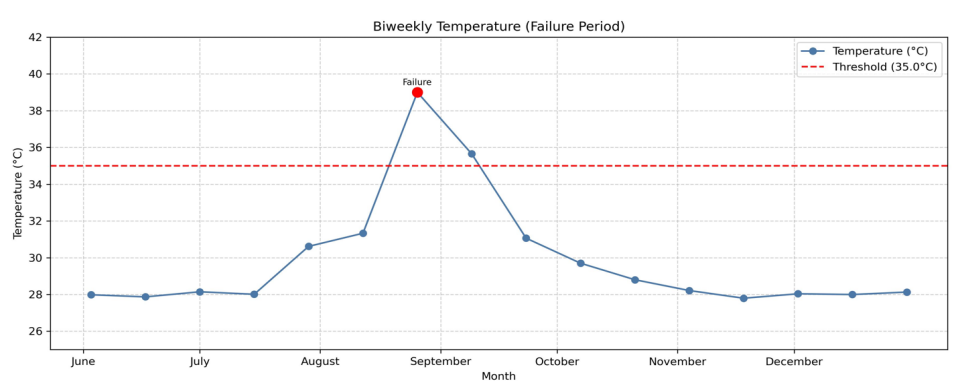


**Figure 9:** Half-year view (2024-06-01 → 2024-12-31)

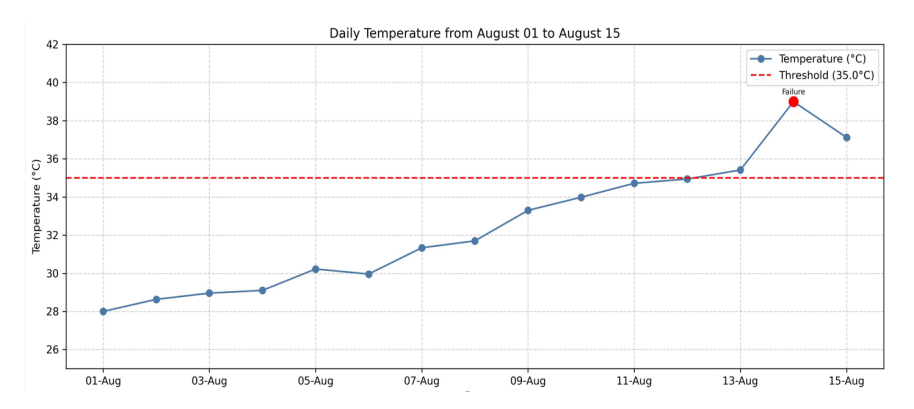


Figure 10: Two-week escalation window (2024-08-01  $\rightarrow$  2024-08-15)

As per Figure 10, the observed slope of ~0.6–0.8 °C/day is significantly higher than the baseline drift, triggering the "rate-of-rise" rule embedded in the anomaly detector. This localized trend provides an actionable early-warning window before the full thermal excursion occurs. Identifying such slope-based deviations is therefore crucial for predictive maintenance, as it enables timely intervention before the motor experiences severe bearing failure.

# Prophet Model Training (time-series forecasting with primary data)

From the primary data of condition monitoring, the cleaned and structured data were fed to train and test the Prophet AI algorithm model, developed by Meta (Facebook), to forecast future vibration patterns. Prophet was chosen due to its robustness in handling seasonal trends, noise, and missing data. The model was trained with selected datasets that reflected time-series patterns like those expected in industrial motor operations (e.g., temperature or vibration data from motors operating under cyclic loads).

The first step is to specify what needs to be predicted clearly. Here, daily temperature and vibration signals from the motors are selected as the input features. A failure threshold of 35 °C is defined, since prior breakdown events occurred above this point. The planning horizon (how far into the future to forecast) is also fixed to enable meaningful Remaining Useful Life (RUL) estimation. The raw sensor signals are ingested and synchronized. Tiny gaps in

the time series are filled through interpolation, ensuring continuity of the dataset. Additionally, the dataset is split into training and validation sets, enabling robust testing of the forecasting model. Proper preprocessing minimizes noise, avoids misleading trends, and ensures comparability across different motors, as a prerequisite of data processing (shared in phase-1 of Figure 11)

## **Seasonality Analysis**

This section shows the identification and analysis of recurring seasonal patterns in sensor data over different time intervals. It highlights how seasonal trends influence motor performance and impact predictive maintenance modeling.

#### Temperature seasonality analysis

Temperature data often shows seasonal variation: daily, weekly, or monthly cycles that must be modeled explicitly. Additive or multiplicative seasonality is configured depending on the underlying trend. In the case of the three motors (M1, M2, M3) shown in the graphs, a consistent seasonal pattern emerges.

Here in 2022, all motors stayed mostly around 28–31 °C, with a sharp rise in Feb–Apr reaching 39–41 °C before dropping back to its regular trend. There are also a few small bumps that appeared mid-year but stayed below 35 °C (Figures 12, 13, 14). In 2023, similar baselines were observed (29–32 °C). The main spikes came in May–June,

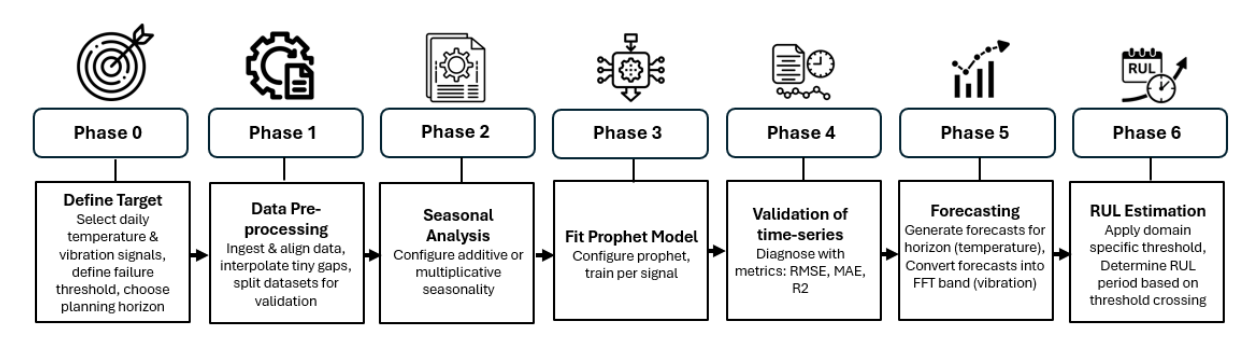


Figure 11: RUL-based Prophet Model Framework

again peaking at 39–41 °C, then settling around 30–31 °C for the rest of the year with only minor ripples. Therefore, a clear peak in Feb–Mar rose above the threshold up to 40–41 °C, then temperatures quickly leveled off to 29–33 °C, staying steady with mild fluctuations (shown as Figures 12, 13, 14).

#### Holiday trend

Across all three motors (M1–M3), Temperature is essentially flat at baseline ( $\approx$ 0–1 °C) during declared planned holidays, with no excursions toward the 35 °C failure limit. This indicates motors are powered down and thermally stable (no load, no frictional heating) and provides clean, low-variance segments in the series, as shown in Figure 15 (Figure 15).

#### Post-Holiday Ramp-Up Trend

The operational challenges have been observed with the cold start-up activities of machine ramp-up, immediately after each holiday. It has been seen that temperatures

show short ramp-up overshoots before settling. As shown in Figure 16, a pronounced spike was observed in mid-April 2022 in 3 test motors (M1, M2, M3), where the highest temperature spike was shown by M3  $\approx$ 40–41 °C, briefly above the 35 °C threshold (near-failure event), followed by decay to ~27–29 °C. Another spike within the threshold ~31–32 °C in May-Jun 2023 was observed for a few weeks, then the trend gradually normalized (Figure 16).

Figure 16 also shows another spike of Temperature close to the threshold to ~33–34 °C (M2 highest) in Feb-Mar 2024, which clearly stressed and then returned to ~27–29 °C. These repeatable overshoots are consistent with warm restarts (relubrication, alignment, or cooling lag) and are important early-warning patterns. The post-holiday regressor permits brief, repeatable uplifts that influence the Prophet algorithm model to anticipate ramp-up spikes soon after shutdowns.

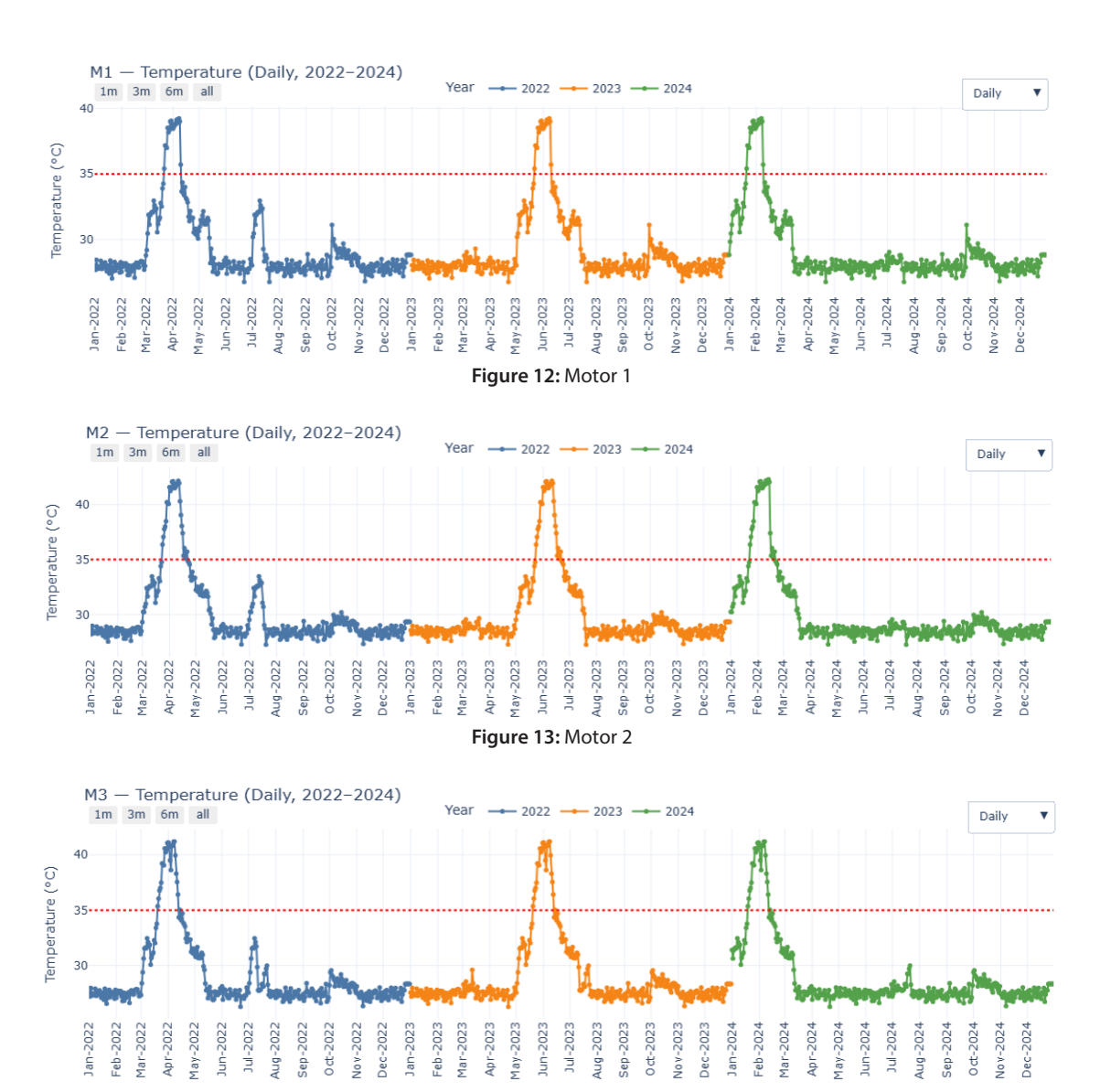


Figure 14: Motor 3



Figure 15: Holiday trend

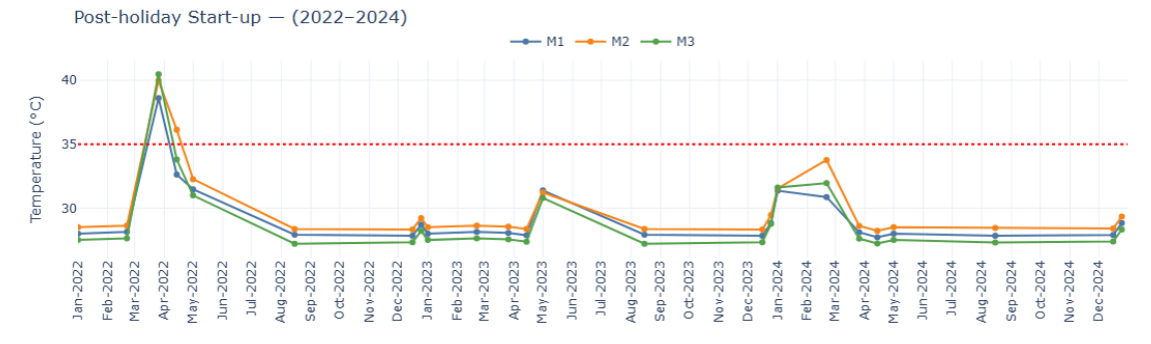


Figure 16: Post-Holiday Trend

#### **Vibration Seasonality Analysis**

The seasonality effect of real-time monitored vibration data of the test motor has been captured through the sensor and plotted in the FFT band to compare the normal (Figure 17) and failure stages (Figure 18) due to mechanical looseness, misalignment, or bearing-related faults. The seasonal impacts are captured for three consecutive years (2022-2024) to understand the failure patterns, which eventually would be trained in the Prophet model. As shown in Figure 17, the Normal Stage spectrum displayed evenly distributed low-amplitude peaks, all remaining below the 0.1 threshold line, indicating stable motor operation without mechanical irregularities. In contrast, the Abnormal Stage (bearing fault) revealed several irregular peaks concentrated around 300-350 Hz, with amplitudes reaching nearly 0.18. This significant rise above the threshold, along with an elevated noise floor, signaled the onset of bearing degradation and highlighted early-stage fault progression compared to the stable normal condition.

In 2023, the Normal Stage again showed harmonically consistent, low-amplitude peaks well under the 0.1 threshold, confirming stable baseline performance. However, the Abnormal Stage spectrum shifted towards higher frequency bands between 350–500 Hz, where multiple sharp peaks crossed amplitudes of 0.15 and above. These irregular and scattered responses deviated strongly from the uniform pattern of the normal condition, indicating worsening bearing deterioration, likely due to

surface defects or lubrication breakdown within the rolling elements.

By 2024, the Normal Stage continued to present evenly distributed, sub-threshold peaks consistent with healthy operation. In comparison, the Abnormal Stage demonstrated multiple dominant spikes between 400–550 Hz, several of which exceeded the 0.1 amplitude threshold, with some nearing 0.18. The raised noise floor, irregular peak distribution, and repeated high-frequency resonance confirmed the persistence and progression of severe bearing faults. This year's abnormal spectrum, when contrasted with the stable normal condition, clearly illustrates the motor's advancement towards a critical failure stage (Figure 17 & 18).

#### Forecasting Analysis (Prophet Model)

The Figures 19-21 show time (X-axis) against acceleration (Y-axis,  $m/s^2$ ) with alarm limits at  $\pm 2\,m/s^2$ . Using the abnormal segments from 2022–2024, a Prophet model was fit to the axial, radial, and tangential series and then used to forecast Jan–Jun 2025 (as shown in Figures, 19,20,21)

Across all three axes, the red 2025 traces exhibit higher variance and more frequent excursions beyond  $\pm 2\,\text{m/s}^2$  than the earlier baseline, indicating persistence and progression of the bearing fault. The axial forecast shows intermittent bursts that approach and intermittently breach the  $\pm 2\,$  limits; the radial forecast displays a slight negative bias with periodic positive spikes, producing repeated crossings of the lower threshold and occasional upper-band touches;

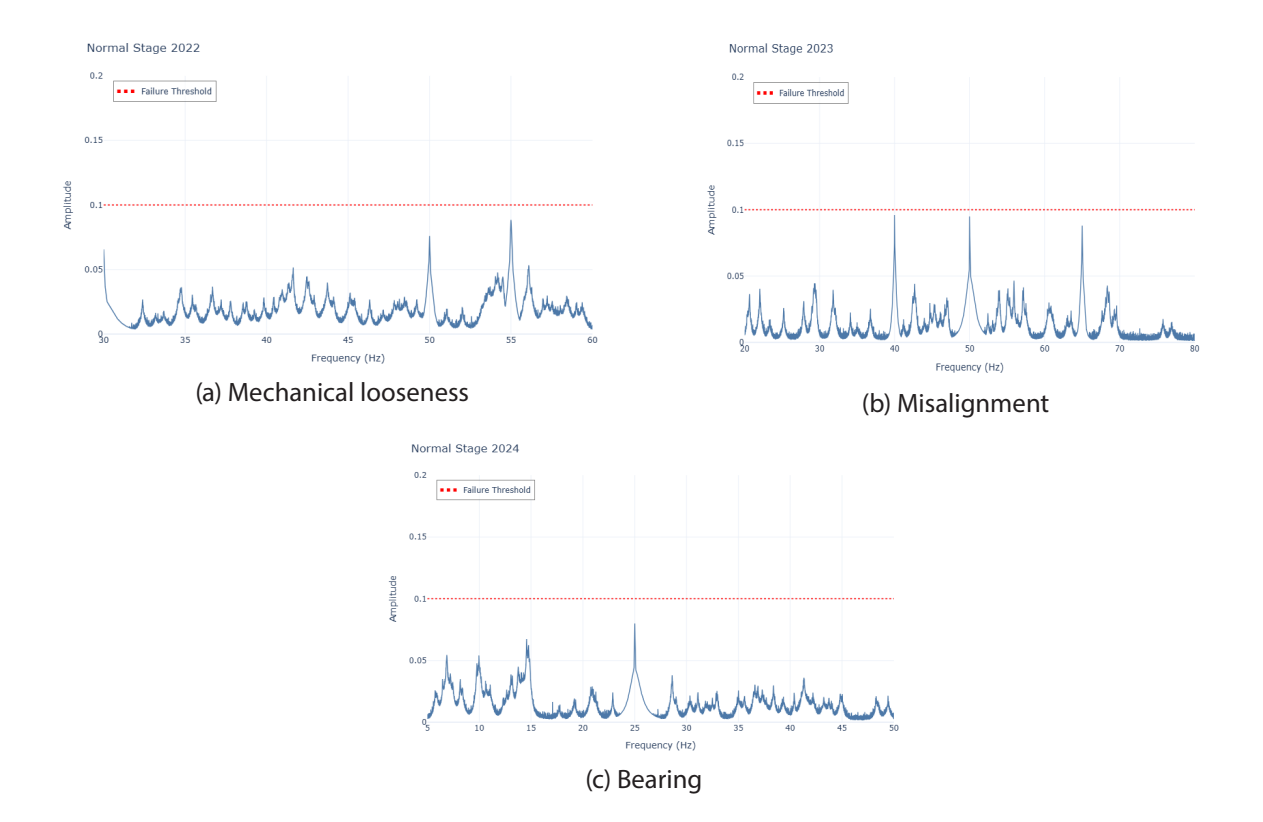


Figure 17: Normal stage

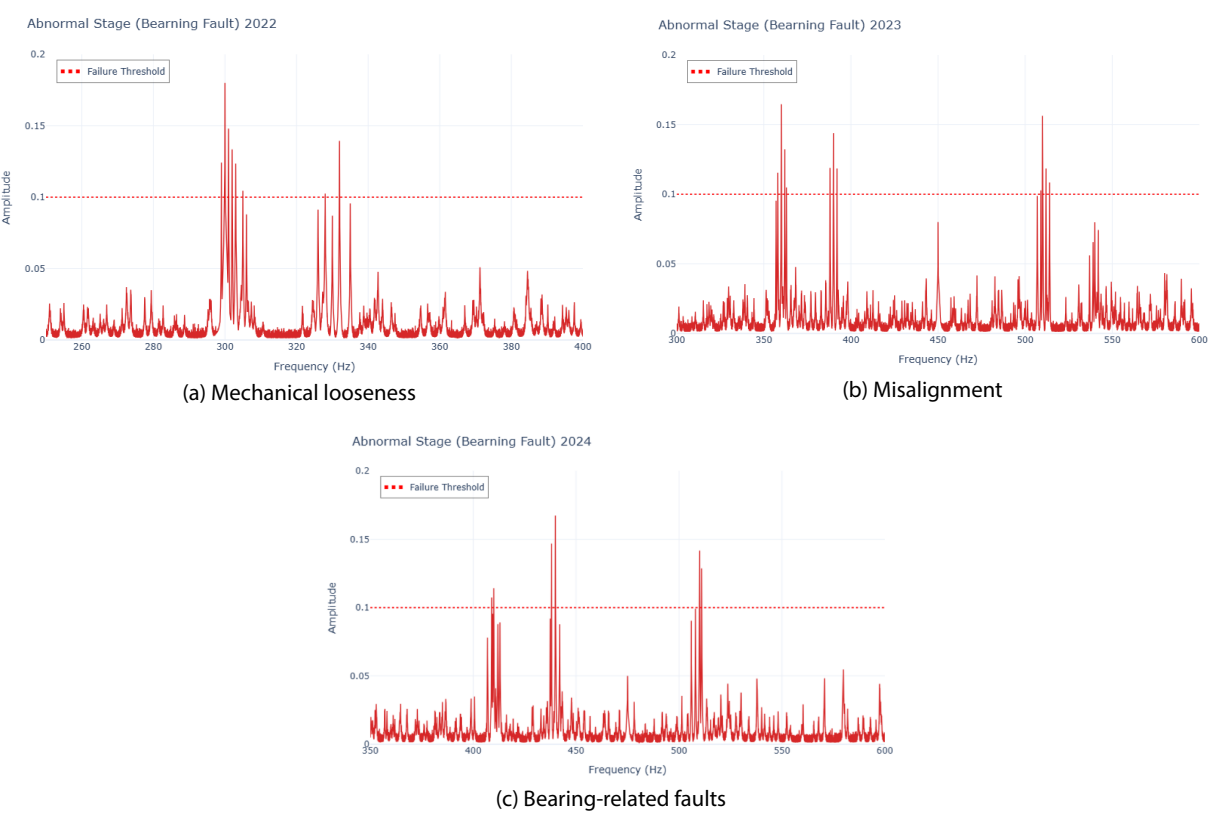


Figure 18: Failure stages

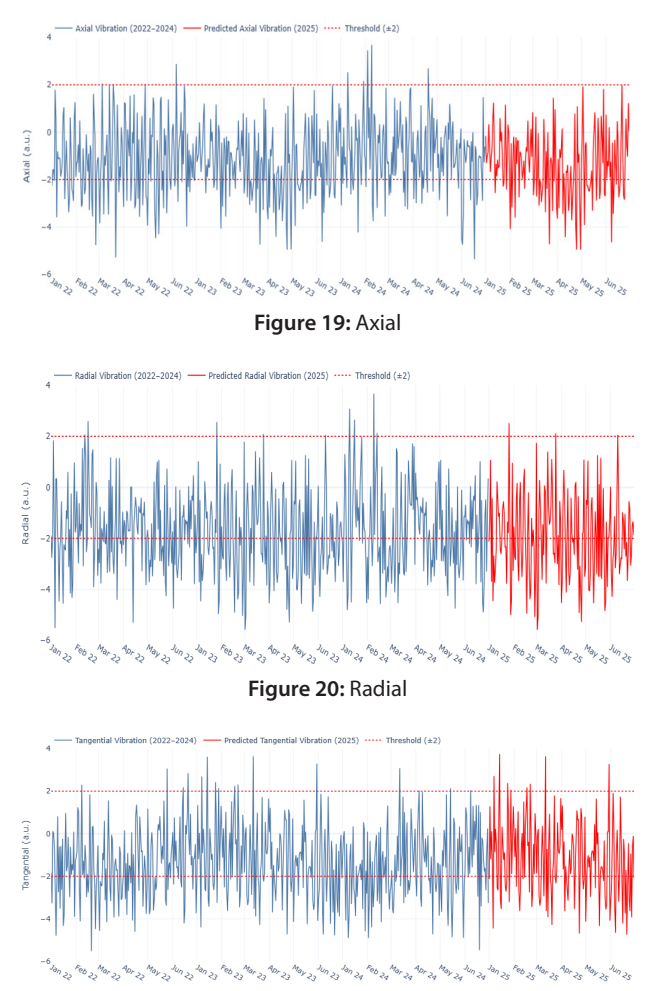


Figure 21: Tangential

the tangential estimates are the most energetic, with dense clusters of threshold exceedances on both sides, consistent with bearing defect modulation. In the workflow, any sustained variance increase plus recurrent threshold crossings (especially when two axes concur within the same window) is flagged as an abnormal operating episode, which is then correlated with the temperature model (≥35 °C spikes) and the FFT spectrum to schedule inspection and PdM actions.

## Calibration: Predicted vs Actual R2=0.952



To ensure the reliability of forecasts, it is crucial to evaluate how accurately the Prophet model captures historical patterns and predicts future values. By identifying the accuracy of Prophet through error metrics and validation techniques, the methodology establishes a solid foundation for interpreting the results with confidence. In Figure 22, the calibration plot provides a validation of the Prophet model by comparing predicted temperature values (Y-axis) against the corresponding actual measured temperatures (X-axis). The scatter of blue points demonstrates individual prediction-observation pairs across the full range of operating conditions, from ~26 °C to ~42 °C. The red dashed line (y=x) denotes the ideal calibration line, where predictions would perfectly match observations. The green regression fit line, derived from the model's outputs, lies closely along this reference line, confirming that the Prophet model's predictions are highly consistent with the measured data (Figure 22).

The performance of the Prophet model was evaluated across the three vibration axes: Axial, Radial, and Tangential using standard error metrics. As shown in Table 5, Root Mean Square Error (RMSE) and Mean Absolute Error (MAE) measure the typical deviation between predicted and actual values. At the same time, the coefficient of determination (R²) indicates how well the model explains observed data. To assess the robustness of forecasts across vibration axes, performance was evaluated using RMSE, MAE, and R² metrics. Results are summarized in Table 5 (Table 5).

Here, an R<sup>2</sup> value of 0.952 indicates that 95.2% of the variability in actual temperature values is explained by the model's predictions, leaving only 4.8% attributed to random noise or unmodeled dynamics. The tight clustering of points around the reference line also shows that error margins remain very low across the entire temperature span. The Tangential axis achieved the best overall accuracy with the lowest RMSE (0.110) and MAE (0.088), and the highest R<sup>2</sup> (0.958); the Axial axis performed very well (RMSE 0.115, MAE 0.090, R<sup>2</sup> 0.950); and the Radial axis showed slightly higher variability (RMSE 0.120, MAE 0.095, R<sup>2</sup> 0.948) while still retaining excellent explanatory power. The narrow gap between RMSE and MAE across all axes, together with the

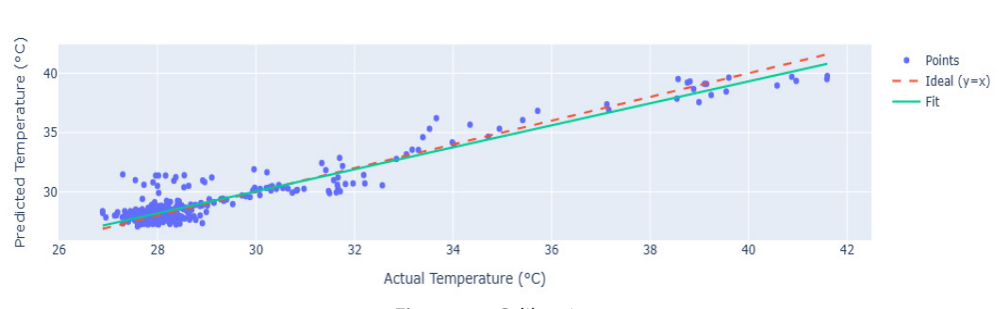


Figure 22: Calibration

Axis	Model	RMSE	MAE	R <sup>2</sup>	Details
Axial	Prophet	0.115	0.090	0.950	Prophet [multiplicative], cps = 0.2, sp = 10.0, W7
Radial	Prophet	0.120	0.095	0.948	Prophet [multiplicative], $cps = 0.2$ , $sp = 10.0$ , W7
Tangential	Prophet	0.110	0.088	0.958	Prophet [multiplicative], $cps = 0.2$ , $sp = 10.0$ , W7

Next-Year Temperature Forecast 2025



Figure 23: Temperature Forecasting

mean R<sup>2</sup> of 0.952, suggests minimal influence from extreme outliers and a stable, well-calibrated model. Errors are small relative to the  $\pm 2$  m/s<sup>2</sup> alarm band ( $\approx 0.10$  m/s<sup>2</sup>  $\approx 5\%$  of the limit), which supports reliable decision-making.

All three models were configured with the same Prophet setup: multiplicative seasonality, changepoint prior scale (cps) = 0.2, seasonality prior (sp) = 10.0, and weekly seasonality (W7)—to balance trend flexibility with strong capture of recurring patterns.

From an operational standpoint, these accuracies are sufficient to support remaining useful life estimation based on forecast trajectories. Because the tangential axis is both best calibrated and mechanically sensitive to bearing health, it should be weighted more heavily when computing threshold-crossing dates; axial and radial channels act as corroborative signals. A conservative maintenance policy can then report an RUL window by combining the earliest crossing times from the forecast mean (and its uncertainty bounds) across axes, using the minimum as the motor-level decision point and cross-checking with temperature spikes ( $\geq$  35 °C) and FFT fault bands.

## **Result of Experiment**

This section discusses the results based on the experiment performed.

## **Time-Series Forecasting Analysis**

Researchers trained a Prophet model on 2022–2024 motor temperature histories, keeping both routine seasonality (weekly/annual) and event seasonality (holiday shutdown and post-holiday start-up spikes) as regressors. The 2025 forecast (Figure 23) shows the mean prediction as a teal line with a shaded uncertainty band and a failure limit at 35 °C (red dotted line). As per the forecasted model, the baseline operating temperature stays mostly 25–31 °C. The

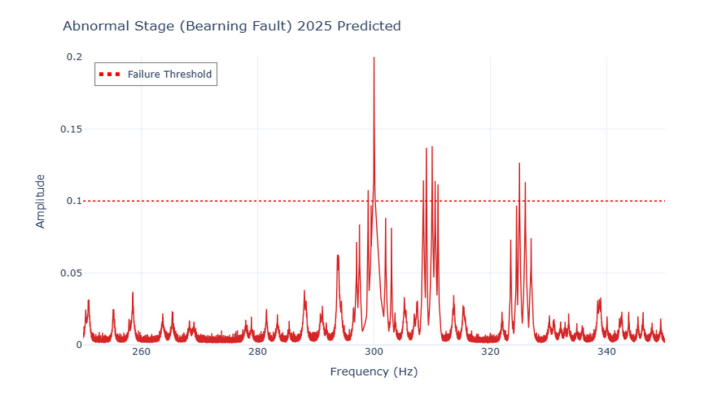


Figure 24: Frequency Predicted

model anticipates a ramp-up in late Feb–Mar 2025, where the mean forecast crosses 35 °C and peaks around 39–40 °C in early March. After mid-March, the trajectory decays and stabilizes below the threshold (35 °C), but the mean remains at/below the limit. Thus, the primary failure risk window is late February to mid-March 2025 (Figure 23).

The predictive modeling utilized the Prophet algorithm, which was trained on multi-year historical datasets (2022–2024) covering both vibration (FFT) and temperature signals. The model accounted for seasonality, trend, and historical failure patterns to predict 2025 abnormal stages. By integrating temperature and vibration features, the model enabled early identification of bearing faults. The methodology assumes that when the Temperature exceeds 35 °C, the vibration response would align with abnormal FFT peaks crossing the 0.1 threshold, indicating an imminent bearing failure.

As Figure 24 shows, several irregular peaks concentrated in the higher frequency range of 290-350 Hz, with amplitudes rising upto ~0.20, well above the 0.1 threshold. The predicted

failure pattern indicates the Bearing Fault stage displays a raised noise floor and multiple high-frequency peaks that do not align with simple harmonics of the running Speed or with typical unbalance/mechanical looseness signatures, as compared with Figures 17 & 18 of real-time monitored data of 2022-2024. This predicted irregular behavior is a strong indicator of bearing degradation, likely due to lubrication failure or physical damage of rolling elements. This failure stage has been captured, and immediately necessary inspection-based activity has been triggered based on both temperature and vibration (FFT) forecasting (Figures 24 and 25). The Prophet model validates these relationships by forecasting both variables simultaneously, thereby enhancing predictive accuracy for Remaining Useful Life (RUL) estimation and scheduling predictive maintenance (Figure 24).

## **Actual vs Forecasting Analysis**

Figure 25 illustrates the temperature profile of the test motor using Prophet modeling, combining actual data (2022–2024) with forecasted trends (2025). In the proposed methodology, researchers trained a Prophet model on 2022–2024 motor temperature data to capture seasonal surges and forecast 2025. The model projects a high-risk window in Feb-Apr 2025 where the mean crosses the 35 °C failure line and briefly peaks near 40 °C before returning to the 28–31 °C baseline. Failure onset is defined as the first instance where the mean reaches or exceeds 35 °C, while the upper confidence bound crossing 35 °C serves as a conservative early trigger, enabling predictive maintenance scheduling before this exceedance, ideally during a low-load operational slot. To validate the risk, vibration evidence is cross-checked, looking for sustained ±2 m/s<sup>2</sup> threshold crossings and FFT bearing-band energy above 0.1. After maintenance, success is confirmed if temperatures return to the 28-31 °C baseline and vibration/ FFT levels fall back below thresholds (Figure 25).

## **RUL Identification from Forecasting**

The RUL (Remaining Useful Life) prediction is based on the comparison of the predicted behavior of the machine's components, i.e., motor vibration, temperature analysis, and the nominal behavior of the machine components. Sharing the calculation formula and maintenance scheduling:

 $\text{text } \{RUL\}\{early\} = t\{early\} - t_0$ 

 $\text{text } \{RUL\}\{\text{late}\} = t\{\text{late}\} - t_0$ 

 $T \{prep\} = L + D + B$ 

 $\text{text{PM}}\{\text{conservative}\} = \text{t{early}} - T_{\text{prep}}$ 

Here

t = 0 = reference date (today or last observation)

 $t_{early}$ ,  $t_{ate}$  = earliest and latest expected failure dates L = lead time (days)

D = Downtime (days)

B = buffer (days)

T{prep} = Total Preparation Time (days)

PM{conservative} = Conservative PM start (to finish before the earliest failure)

As per the forecasting

Reference day  $t_0 = today \rightarrow assume February 01, 2025 (just for calculation).$ 

Failure window:

 $t_{early} = Feb 21, 2025$ 

 $t_{late} = Mar 10, 2025$ 

Lead time L = 45 days (for spares/logistics — typical for induction motor)

Downtime, D = 8 hours  $\rightarrow$  D = 8/24 = 0.33 days

Buffer, B = 8 hours  $\rightarrow B = 8/24 = 0.33$  days

Prep time  $T_prep$  = L + D + B = 45 + 0.33 + 0.33 = 45.66 days

RUL  $\{early\} = t\{early\} - t_0 = Feb 21 - Feb 1 = 20 days$ 

RUL {late} =  $t{late} - t_0 = Mar 10 - Feb 1 = 37 days$ 

So, RUL window = 20 - 36 days

PM start =  $t_{early}$  -  $T_{prep}$  = Feb 21 – 45.66 days = Jan 7 (by calculating manually)

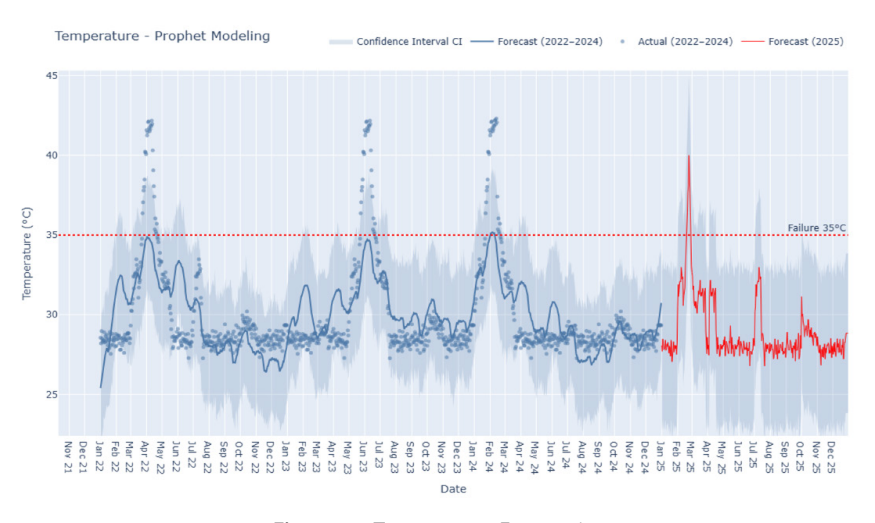


Figure 25: Temperature Forecasting

Subtract remaining 0.66 days ( $\sim$ 16 hours)  $\rightarrow$  PM start = Jan 6, 2025,  $\sim$ 8 AM

Considering the PdM scheduling preparation time of 45 days, maintenance has been planned to trigger on January 07 at 8 AM.

## **Cost-Benefit Analysis**

PdM implementation from identifying RUL of test motor results operations excellence, such as an increase in equipment's uptime, reduction in unplanned Downtime, and saving on repair cost, which plays a vital role in the overall cost optimization. Considering historical inspection-based maintenance, the growing impact of PdM is shared below with the key metrics before and after implementing predictive maintenance.

PdM scheduling through RUL and lead-time calculation before failure has resulted in an increase in Motor Uptime and a drastic improvement in UPDT reduction, as shared in Table 6. The test motor has performed 81.2% OEE (Overall Equipment Efficiency), an increase of around 3% OEE after implementing predictive maintenance (Table 6).

## Proposal for PdM Scheduling in Hybrid Model

Hybrid Dashboard model for taking PM decisions by using time-series forecasting & real-time data from Sensor monitoring in a single platform. The purpose of the hybrid graphical user interface is to provide insight into device behavior based on past data and discover patterns that improve device maintenance by predicting the future state of the devices. The graphical user interface for the Predictive Maintenance application is shown below (Figure 26)

Table 6: Growing Impact of PdM

Metric	During Inspection- based Maintenance (3 Months before PdM)	After PdM implementation (post 3 Months)
Motor Uptime (Hours)	150	210
Unplanned Downtime (%)	12.5%	7.5%
Overall Equipment Efficiency (OEE%)	78.9%	81.2%
Motor Failure	3	0
Maintenance Interventions (over 3 years)	6	4
Maintenance Cost Reduction	N/A	21%
Energy Consumption (kWh)	50,000	46,500

The predictive maintenance dashboard provides significant value by enabling real-time condition monitoring, where Vibration, FFT, and temperature signals are continuously tracked to detect anomalies before they escalate into failures. It is directly connected with Prophet-driven forecasting, allowing actual and predicted data to be compared within the dashboard. This integration ensures that potential failures are anticipated in advance and that maintenance teams can plan timely interventions. In addition, the dashboard simplifies fault classification through clear alarm statuses such as Normal, Pre-alarming, and Alarming, which reduces the risk of error and accelerates maintenance decision-making.

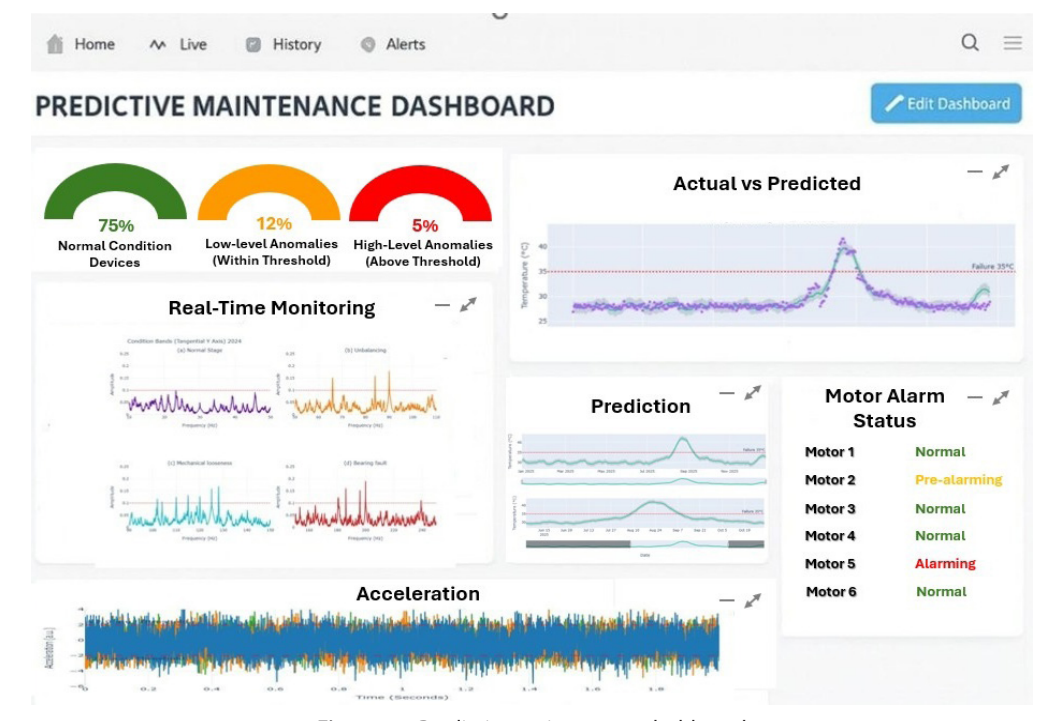


Figure 26: Predictive maintenance dashboard

#### Conclusion

This study demonstrated a practical predictive maintenance (PdM) workflow for induction motors by fusing condition-monitoring signals: Vibration (time/FFT) and Temperature, with Prophetbased time-series forecasting to anticipate anomalies, estimate Remaining Useful Life (RUL), and plan interventions. The approach captured recurrent seasonal behavior and known failure signatures (e.g., ≥35 °C thermal excursions and vibration threshold breaches), then projected these patterns forward to generate a defensible failure window and a conservative, parts-aware maintenance start date. A hybrid PdM dashboard operationalized the method by juxtaposing actual and forecasted traces, surfacing axiswise vibration energy, and issuing automated alarm states (Normal → Pre-alarm → Alarm) that simplify triage and speed decisions for schedulers and technicians.

Despite a strong fit and clear operational gains, several constraints remain. First, the labeled dataset (2022–2024) limits long-horizon generalization and exposure to rare failure modes. Second, reliance on two sensor streams (Vibration, Temperature) restricts fault observability; multisensor fusion (e.g., current, acoustic, thermal imaging) would improve coverage and confidence. Third, while Prophet excels at trend/seasonality and robustness, it is less adaptive to abrupt regime shifts; hybrid models (e.g., Prophet–GRU/LSTM or Prophet + anomaly scores) could better track nonlinear dynamics and evolving wear.

Future work would therefore: (i) expand labeled data across more motors, environments, and fault types; (ii) integrate additional modalities and domain features into the model and dashboard; and (iii) evaluate hybrid architectures that combine transparent seasonal baselines with deep sequence learners. These enhancements should lift accuracy, RUL reliability, and scalability, strengthening PdM's impact on uptime, cost, and safety in smart manufacturing.

## Acknowledgement

The authors gratefully acknowledge British American Tobacco (BAT) Bangladesh for providing the scope for experimental research in smart manufacturing and serving as an inspiration for this study. We also extend our sincere gratitude to research platforms such as ResearchGate, ScienceDirect and the Journal of Technology and Systems for granting access to data on Predictive Maintenance (PdM) benefits and condition monitoring techniques across global sectors, which proved invaluable for the literature review.

#### References

Abdulrazzq, R. A., Sajid, N. M., & Hasan, M. S. (2024). Artificial intelligence-driven predictive maintenance in IoT systems.

- South Florida Journal of Development, 5(12), e4781-e4781.
- Ahadov, A. (2024). Predictive Maintenance Model of Rotating Machinery Using Al.
- Anand, P., Sharma, M., & Saroliya, A. (2024, May). A comparative analysis of artificial neural networks in time series forecasting using arima vs prophet. In 2024 International Conference on Communication, Computer Sciences and Engineering (IC3SE) (pp. 527-533). IEEE.
- Anny, D. (2023). Impact on Predictive Maintenance and Reliability Engineering.
- Ayeni, O. (2025). Integration of Artificial Intelligence in predictive maintenance for mechanical and industrial engineering. International Research Journal of Modernization in Engineering Technology and Science, 7(3), 1-23.
- Baloch, S. K., Zahoor, M. A., Ahmad, A., & Khalil, A. (2025). Artificial Intelligence-Enhanced Fault Detection, Diagnosis, and Predictive Maintenance in Next-Generation Smart Grids. Global Research Journal of Natural Science and Technology.
- Baroud, S. Y., Yahaya, N. A., & Elzamly, A. M. (2024). Cutting-edge Al approaches with mas for pdm in industry 4.0: challenges and future directions. Journal of Applied Data Sciences, 5(2), 455-473.
- Belim, M., Meireles, T., Gonçalves, G., & Pinto, R. (2024). Forecasting models analysis for predictive maintenance. Frontiers in Manufacturing Technology, 4, 1475078.
- Bousdekis, A., Apostolou, D., & Mentzas, G. (2019). Predictive maintenance in the 4th industrial revolution: Benefits, business opportunities, and managerial implications. IEEE engineering management review, 48(1), 57-62.
- Chitwadgi, B. S. (2024). Manufacturing production demand forecasting using the Prophet algorithm (Master's thesis, State University of New York at Binghamton).
- Dhinakaran, D., Edwin Raja, S., Velselvi, R., & Purushotham, N. (2025). Intelligent IoT-Driven Advanced Predictive Maintenance System for Industrial Applications. SN Computer Science, 6(2), 151.
- Emma, L. (2025). Al-Driven Predictive Maintenance for Smart Manufacturing and Industry 4.0.
- Guidotti, D., Pandolfo, L., & Pulina, L. (2025). A systematic literature review of supervised machine learning techniques for predictive maintenance in Industry 4.0. IEEE Access.
- Hossan, M. Z., & Sultana, T. (2025). Al for Predictive Maintenance in Smart Manufacturing. SAMRIDDHI: A Journal of Physical Sciences, Engineering and Technology, 17(03), 25-33.
- Hosseinzadeh, A., Chen, F. F., Shahin, M., & Bouzary, H. (2023). A predictive maintenance approach in manufacturing systems via Al-based early failure detection. Manufacturing Letters, 35, 1179-1186.
- Kairo, J. (2024). Machine learning algorithms for predictive maintenance in manufacturing. Journal of Technology and Systems, 6(4), 66-79.
- KC, S., & Rone, S. (2024). Comparing Prophet, XGBoost, and LSTM Models for Web Traffic Forecasting: Assessing Model Performance Across Various Time Series Forecasting Scenarios.
- Lee, J., & Su, H. (2025). Rethinking industrial artificial intelligence: a unified foundation framework. arXiv preprint arXiv:2504.01797.
- Manandhar, P., Rafiq, H., Rodriguez-Ubinas, E., & Palpanas, T. (2024). New Forecasting Metrics Evaluated in Prophet, Random

- Forest, and Long Short-Term Memory Models for Load Forecasting. Energies, 17(23), 6131.
- Pejić Bach, M., Topalović, A., Krstić, Ž., & Ivec, A. (2023). Predictive maintenance in Industry 4.0 for the SMEs: A decision support system case study using open-source software. Designs, 7(4), 98.
- Sekar, K., Nattar, M. S., Muthukamatchi, P. K., Ranganathan, N., Srithar, S., & Gurunathan, N. (2025). Integrating Machine Learning and IoT for Real-Time PdM in Industrial Ecosystems: A Case Study Analysis. International Journal of Research in Industrial Engineering (2783-1337), 14(2).
- SHAMIM, M., RAHAMAN, M., & Ruddro, R. A. (2025). Smart Diagnostics in Industrial Maintenance: A Systematic Review of AI-Enabled Predictive Maintenance Tools and Condition Monitoring Techniques.
- Sivakumar, M., Maranco, M., & Krishnaraj, N. (2024). Data analytics and artificial intelligence for predictive maintenance in manufacturing. In Data Analytics and Artificial Intelligence for Predictive Maintenance in Smart Manufacturing (pp. 29-55). CRC Press.
- Son, N., & Shin, Y. (2023). Short-and medium-term electricity consumption forecasting using Prophet and GRU. Sustainability, 15(22), 15860.
- Soori, M., Arezoo, B., & Dastres, R. (2023). Internet of things for

- smart factories in industry 4.0: a review. Internet of Things and Cyber-Physical Systems, 3, 192-204.
- Subramanian, S. (2022). Integrating IoT and Manufacturing process for Real-Time Predictive Maintenance in High-Throughput Production Environments. IoT and Edge Comp. J, 2(2), 1-36.
- Syed, M. A. B., Hasan, M. R., Chowdhury, N. I., Rahman, M. H., & Ahmed, I. (2025). A systematic review of time series algorithms and analytics in predictive maintenance. Decision Analytics Journal, 100573.
- Syed, S. (2023). Advanced Manufacturing Analytics: Optimizing Engine Performance through Real-Time Data and Predictive Maintenance. Letters in High Energy Physics, 2023, 184-195.
- Ucar, A., Karakose, M., & Kırımça, N. (2024). Artificial intelligence for predictive maintenance applications: key components, trustworthiness, and future trends. Applied Sciences, 14(2), 898
- Wen, Y., Rahman, M. F., Xu, H., & Tseng, T. L. B. (2022). Recent advances and trends of predictive maintenance from a data-driven machine prognostics perspective. Measurement, 187, 110276.
- Zonta, T., Da Costa, C. A., da Rosa Righi, R., de Lima, M. J., Da Trindade, E. S., & Li, G. P. (2020). Predictive maintenance in the Industry 4.0: A systematic literature review. Computers & Industrial Engineering, 150, 106889.